Patil *et al.*
Future Journal of Pharmaceutical Sciences (2023) 9:109
https://doi.org/10.1186/s43094-023-00560-7

Future Journal of Pharmaceutical Sciences

RESEARCH Open Access

Peptide-modified PAMAM-based bone-targeting RNA delivery system

Suryaji Patil[1,2,3†], Yong-Guang Gao[4†] and Airong Qian[1,2,3*]

Abstract

Background Osteoporosis, among other bone diseases, has become a prevalent cause of decreased quality of life in older and postmenopausal women. Traditional anti-osteoporotic therapies, though widely prescribed, are limited by a lack of cell- or tissue-specific targeting ability and effectiveness without side effects. Gene therapy is rapidly replacing traditional therapeutics, primarily because of its specific targeting ability and efficiency. Among viral- and non-viral-based gene therapies, the latter is often preferred over the former due to lower cytotoxicity, immunogenicity, and ease of modification with different molecules to improve efficiency and extend gene expression. We designed and synthesized a multifunctional bone-targeting ribonucleic acid (RNA) delivery system based on polyamidoamine (PAMAM). PAMAM was modified with the serine-aspartate-serine-serine-aspartate (SDSSD) peptide to deliver antagomir 138-5p to osteoblasts (MC3T3-E1 cell line) in vitro and in vivo using the ovariectomized (OVX) mouse model.

Results The results showed that this system was less cytotoxic than polyethylenimine (PEI) and could bind to RNA favorably while maintaining gene delivery ability in vitro. In vivo data showed that the distal tibia and femur of the mice in the PAMAM-SDSSD (PS) + RNA group had improved bone mineral density (BMD), bone mineral content (BMC), and bone volume compared to those in the PS + Negative Control (NC) or OVX groups. Moreover, the femurs of the PS + RNA group mice demonstrated a higher breaking point, stress, stiffness, and elasticity than those of the PS + NC or OVX mice, suggesting improved femur strength in the OVX mice treated with RNA delivered through SDSSD-modified PAMAM.

Conclusion This study shows that SDSSD modification of PAMAM not only improves gene delivery capacity but also enhances the cell targeting efficiency of nanoparticles towards osteoblasts. The successful delivery of antagomir 138-5p to osteoblasts demonstrates cell-specificity and gene delivery to alleviate osteoporotic symptoms.

Keywords Peptide, PAMAM, Bone-targeting, Gene therapy, RNA therapeutics, Osteoporosis

† Suryaji Patil and Yong-Guang Gao have eqaully contributed to this work.

*Correspondence:
Airong Qian
qianair@nwpu.edu.cn
[1] Laboratory for Bone Metabolism, Key Laboratory for Space Biosciences and Biotechnology, School of Life Sciences, Northwestern Polytechnical University, Xi'an 710072, Shaanxi, China
[2] Research Center for Special Medicine and Health Systems Engineering, School of Life Sciences, Northwestern Polytechnical University, Xi'an 710072, Shaanxi, China
[3] NPU-UAB Joint Laboratory for Bone Metabolism, School of Life Sciences, Northwestern Polytechnical University, Xi'an 710072, Shaanxi, China
[4] Tangshan Key Laboratory of Green Speciality Chemicals, Department of Chemistry, Tangshan Normal University, Tangshan 063000, China

Background

Bone disorders such as osteosarcoma, Paget's disease, osteoarthritis, and osteoporosis have become major disorders that affect millions around the world. Among these, osteoporosis is the most common, affecting more women than men, and can significantly increase morbidity, financial costs, and even mortality [1]. Osteoporosis is characterized by decreased bone strength and integrity as a result of compromised bone microstructure, which increases the risk of fractures such as spine, hip, and forearm fractures, but hip fractures have the most devastating impact on life. In general, the situation is associated

with older people and postmenopausal women [2]. The main causal link to osteoporosis is the disruption of bone remodeling, a highly coordinated process of osteoblast-mediated bone formation and osteoclast-mediated bone resorption mediated by hormones and signaling proteins [3]. Genetics, age, smoking, inadequate intake of calcium and vitamin D, and other diseases contribute to the progression of osteoporosis, but estrogen deficiency is the major contributing factor in osteoporosis in postmenopausal women [4]. Dual-energy X-ray absorptiometry (DXA) is generally performed for the diagnosis of osteoporosis and to chart the next course of treatment. The existing osteoporosis treatments include chemical as well as biological agents and function as anti-resorptive agents. The chemical agents include bisphosphonates, while estrogen and selective estrogen receptor modulators (SERMs), parathyroid hormone (PTH) and PTH-related peptide (PTHrP), denosumab, and odanacatib constitute biological agents [5, 6]. However, due to their side effects and low efficiency, alternative therapies such as gene therapy have become highly sought-after therapeutics.

Usually, viral- and non-viral-based agents are employed for gene delivery. Although viral-based vectors have a high transfection rate, the emergence of pre-existing immunity, a virus-induced immunogenic response, genome integration, and payload size limitations, restrict their wider exploitation [7, 8]. Non-viral vectors, on the other hand, have become the preferred alternative as gene vectors for medical purposes due to their bicompatibility, low immunogenicity, and low mutagenic effects [9, 10]. Nevertheless, they lack greater targeting efficiency, specificity, and prolonged gene expression, which minimizes their utilization in preclinical and clinical studies [11]. Among non-viral-based substances such as cationic lipids, cationic and engineered polymers, nanoparticles, etc., cationic polymers, due to their simplicity in production, controllable chemical composition, and chemical flexibility, have become popular choices to facilitate nucleic acid transfer [12, 13]. Linear or branched polyethylenimine (PEI) is regarded as an ideal cationic polymer candidate for non-viral gene delivery because of the abundance of amine groups on the surface, which not only provides a greater surface for nucleic acids but also allows the synthesis of hybrid molecules [14]. However, its non-specific interactions with blood components, the extracellular matrix, and off-target cell effects have made it necessary to find alternative polymers. As an alternative to PEI, dendrimers can be used as gene vectors because of their branching structure, uniform size, versatility, selectivity for biological targets, and ability to improve the solubility and stability of the payload [15]. Their branched structure provides a large surface for drug encapsulation either through non-covalent interaction or through covalent coupling, and they can be modified according to the chemical nature of the payload. These have shown promising effects in anti-neoplastic, anti-inflammatory, antiviral, and imaging diagnostic therapies [16, 17].

Polyamidoamine (PAMAM) is one such dendrimer that can be used to carry genes and allows greater flexibility in alterations, such as the addition of target-specific moieties. These are synthesized through a series of sequential reactions known as "generations" (G), which can be controlled to achieve uniform size. The high-density cationic charges on their surface electrostatically interact with nucleic acids (DNA and RNA), forming complexes that effectively deliver genes in vitro and in vivo [18]. PAMAM dendrimers of Generations 5 and 6 (G5 and G6) have been described as effective in vitro gene delivery systems; however, their poor in vivo efficacy and high cytotoxicity have been setbacks. These drawbacks can be overcome by modifying PAMAM with different molecules. Polyethylene glycol (PEG), arginine-glycine-aspartate (RGD), alkyl-carboxylate chain, and cholesteryl chloroformate-based modifications of PAMAM have been shown to considerably improve biocompatibility and hemocompatibility by reducing RBC aggregation and enhance transfection efficiency [19–21]. Because of their ability to provide real-time monitoring as well as non-invasiveness, nanoparticles can also be labeled with fluorescent moieties. Among the various fluorescent moieties, amine-attached 1,8-naphthalimide cores have the potential to be useful as lysosome staining agents, efficient non-viral gene delivery vectors, and fluorescent sensors for live animal imaging [22–25].

Because its successful clinical applications can significantly advance the treatment of bone injuries and disorders, bone-targeted drug delivery is a new area for research. As potential moieties for targeted delivery systems, molecules with a high affinity for bone, low systemic concentrations, and a propensity to remain in the bone tissue for an extended period of time have been investigated [26]. Previous studies have shown that the addition of small molecules like repeating sequences of amino acids and aptamers can improve the polymer's ability to target specific bone cells in bone tissue [27]. However, their use as bone formation surfaces may be restricted due to their preference for bone resorption surfaces and highly oriented hydroxyapatite crystals [28–30]. Given the advancements in finding new long noncoding RNAs (lncRNAs), small interfering RNAs (siRNAs), microRNAs (miRNAs), and antisense oligonucleotides (ASOs) in bone tissue and osteoporosis, significant improvements have been made in the identification of new targets and potential therapeutics for

gene therapies [31–33]. RNA-based gene silencing, as opposed to pDNA-based gene silencing, has become the preferred method for preventing antagonistic genes from being expressed in osteoporosis [34]. The most significant barrier to developing an efficient bone-targeted gene delivery system, however, remains the safe and efficient delivery of RNA to specific bone cells with no or limited circulation in other tissues [35, 36]. (DSS)6 or SDSSD peptides added to the surface of polymers have been shown to improve gene delivery to specific bone cells and, as a result, bone architecture, indicating their capability as targeting and non-viral gene vectors [30, 37].

However, a multifunctional delivery system that can deliver a gene, provide live monitoring in study animals, and have a strong preference for a specific cell or tissue has not yet been reported. By combining the capabilities of PAMAM, a strong cationic nucleic acid binding polymer, 4-amino-1, 8-naphthalic anhydride as a fluorescent probe, and SDSSD peptide as a targeting moiety towards osteoblasts, we designed a novel multifunctional delivery system to effectively and specifically deliver RNA to bone tissue in the hope that it will offer an alternative to conventional bone therapeutics.

Materials

Materials

Polyamidoamine (PAMAM (G5), Mw: 28,826) was provided by Weihai Chenyuan Molecular New Materials Co., Ltd. (China), amino and hydroxyl groups protected bone-targeting peptides were procured from Jill Biochemical (Shanghai) Co., Ltd. Polyethylenimine hydrochloride (PEI, linear, average Mn 20,000, PDI ≤ 1.2) was obtained from Sigma-Aldrich (USA). Lipofectamine™ 2000 (Lipo™ 2000) was purchased from Thermo Fisher Scientific (USA). 4-amino-1,8-naphthalic anhydride was obtained from Ruixibio (Xi'an, China). 1-hydroxybenzotriazole (HOBt), dimethyl sulfoxide (DMSO), and 1-ethyl-3-(3-dimethylaminopropyl) carbonyldiimide hydrochloride (EDCl) were purchased from Beijing Ouhe Technology Co. Ltd. (Beijing, China). Diisopropylethylamine (DIPEA), triethylamine, p-methylphenol, pentobarbital sodium, and 3-(4, 5-dimethylthiazolyl-2)-2, 5-diphenyltetrazolium bromide (MTT) was purchased from Beijing Solarbio Science & Technology Co., Ltd. (Beijing, China), trifluoroacetic acid (TFA) was obtained from Beijing Coupling Technology Co., Ltd. MiR 138-5p (antagomir (5'CGGCCUGAUUCACAACACCAGCU3') and NC (F-5'AGCUGGUGUUGUGAAUCAGGCCG3' R-5'UCGACCACAACACUUAGUCCGGC3') were obtained from GenePharma (Shanghai, China), and EGFP siRNAs (F-5'GGCUACGUCCAGGAGCGC ACC3′ R-5'UGCGCUCCUGGACGUAGCCUU3′) were obtained from GenePharma (China). Primers were synthesized and obtained from TsingKe (Beijing, China). RNA in this article refers to the antagomir 138-5p unless specified. As a solvent for chemical preparation, milli-Q grade distilled and deionized water was used in all experiments.

Synthesis

Dendritic molecule polyamidoamine G5 (1.0 equivalents (eq)) and 4-amino-1,8-naphthalic anhydride (10 eq) were dissolved in 1 ml of ethanol solution, stirred for 0.5 h at room temperature, heated for 8 h, and dialyzed for 48 h to obtain compound 1. In this article, we referred to this compound 1 as P. Naphimide-modified compound 1 (1.0 eq) was dissolved in the mixture of EDCI (80 eq), HOBt (80 eq), and DIPEA (80 eq) with 80 equivalents of amino and hydroxyl-protected bone-targeted peptides in 2 ml of dichloromethane for 24 h. After the end of the reaction, the mixture was dialyzed for 48 h to obtain compound 2. Compound 2 was dissolved in 2 ml of TFA at room temperature for 24 h and dialyzed for 48 h to obtain the final compound (compound 3) (Fig. 1A). In this article, we referred to this compound 3 as PS (PAMAM-SDSSD).

Characterization

Scanning electron microscopy (SEM)

The morphology of particles was determined by scanning electron microscopy according to a previously established protocol [38]. Briefly, 1 µl of antagomir 138-5p (200 µg/mL) was mixed with the appropriate volume of PS nanoparticle solution to form complexes and then diluted with water. After incubation at 37 °C for 5 min, complexes were added dropwise onto the silicon slice. The slice was dried at room temperature at atmospheric pressure overnight and then observed under a scanning electron microscope.

^{1}H NMR

The structural composition of compounds was investigated according to the previous protocol [39] through ^{1}H NMR spectra analysis using a Bruker Avance III 400 MHz spectrometer at 25 °C using D_2O as a solvent.

Zeta potential and size

The complex of PS with RNA was prepared by adding 1 µl of antagomir 138-5p (264 µg/ml) to the appropriate volume of the stock solutions of PS. After 30 s of vortexing, the complex solution was diluted with deionized water. The zeta potential and the hydrodynamic size were measured using the Nano-ZS 3600 ZetaPlus Particle Size and Zeta Potential Analyzer (Malvern Panalytical, Worcestershire, UK).

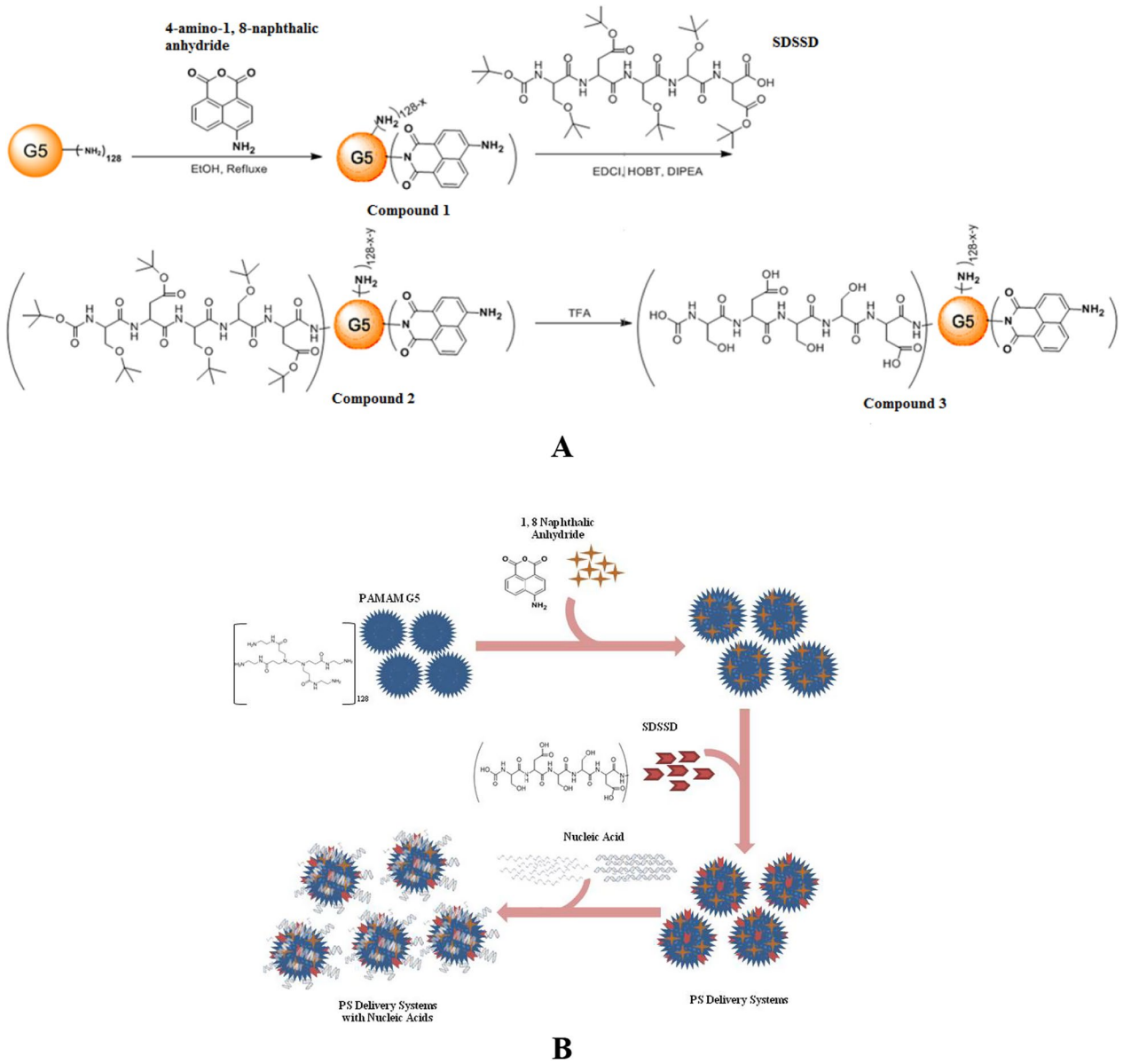

Fig. 1 Design and Synthesis of PS. **A** Chemical synthesis route of PS. **B** Schematic diagram of PS showcasing the design of the nucleic acid delivery system

Gel retardation assay

The different molecular weight ratio complexes of PS with RNA were prepared by adding the appropriate volume of the polymers to 80 nM of antagomir-138-5p. After incubation for 20 min at room temperature, the samples were analyzed using 1% (w/v) agarose gel electrophoresis with Tris–acetate (TAE) as a running buffer for 30 min at 120 V. The bands were visualized using the Gel Doc XR imaging system (BioRad, USA) and processed using Quantity One software.

Cell culture and transfection

The mouse pre-osteoblasts (MC3T3-E1 cells) were cultured in α-Minimal Essential Media (MEM), and mouse leukemic monocyte/macrophage (RAW264.7) (ATCC (Manassas, USA), HEK293-EGFP transgenic cells, and C3H10T1/2 were cultured in Dulbecco's Modified Eagle Medium (DMEM, Gibco™, Thermo Fisher Scientific) media, respectively, supplemented with 10% FBS (Biological Industries, Israel), 100 µg/ml streptomycin, and 100 units/ml penicillin (Amresco, USA) and maintained

at 37 °C, 5% CO_2, and 95% humidity. 0.25% trypsin containing 10 mM EDTA was used for the passage of cells in the experiment.

For cell transfection, MC3T3-E1 or RAW264.7 were seeded at a cell density of 8×10^4 cells cm^{-2} and transfected with antagomir-138-5p or agomir-138-5p (negative control (NC)) only, and with PS and P. The antagomir or NC concentration was 50 nM. After incubation for 6 h, the serum-free medium was replaced by a fresh growth medium containing 10% FBS. 48 h after transfection, cells were harvested for real-time polymerase chain reaction (PCR) or cytotoxicity assays.

Cytotoxicity

The cell viability assay was performed to assess the cytotoxic effect of PEI or PS on MC3T3-E1, RAW 264.7, and C3H10T1/2. Briefly, MC3T3-E1, RAW264.7, and C3H10T1/2 were seeded in the appropriate medium and exposed to various concentrations of PEI, or PS. After treatment for 12 h, the spent medium was replaced with MTT solution (5 mg/ml in PBS), and the plates were further incubated for 4 h in the incubator. After incubation, DMSO was added to each well, and absorbance was measured at 570 nm using a microplate reader (Synergy HT, Bio-Tek, USA).

EGFP gene knockdown experiment

HEK293-EGFP cells were seeded in a 48-well plate at a density of 8×10^4 cells per well in 0.5 ml culture medium and incubated overnight. After reaching 80%-90% confluence, cells were transfected with green fluorescent protein (GFP) siRNA using P, PS, Lipofectamine™ 2000, or PEI polymers for 6 h in serum-free media (siRNA at a final concentration of 120 nM/well). The transfection medium was replaced with a culture medium and cells were incubated for another 24 h. The EGFP expression was measured using fluorescence microscopy. ImageJ software was used to semi-quantify images. P, Lipofectamine™ 2000, and PEI-treated groups served as positive controls.

RNA extraction and real-time quantitative PCR (RT-qPCR)

Total RNA was extracted from cell samples using the Omega Total RNA Kit (Omega, USA) according to the manufacturer's instructions, and RNA quality was determined by ultraviolet (UV) spectrophotometry. 1 μg of total RNA was reverse transcribed into complementary DNA using a cDNA synthesis kit (PrimeScript™ RT Reagent Kit, TaKaRa, Japan) following the manufacturer's instructions. The primer sequence for miR 138-5p reverse transcription was 5'-GTCGTATCCAGTGCAGGGTCCGAGGTATTCGCACTGGATACGACCGGCCT-3'. Real-time quantitative PCR was performed using the SYBR® Premix Ex Taq™ II kit (TaKaRa, Japan) and gene-specific primers (MACF1 F-5′-GAAAACATTCACCAAGTGGGTCAAC-3′, R-5′-TGTCCATCCCGAAGGTCTTCATAG-3'; GAPDH F-5′-TGCACCACCAACTGCTTAG-3′, R-5′-GGATGCAGGGATGATGTTC-3'; miR-138-5p F-5'- GCGGCGGAGCTGGTGTTGTGAATC-3', R-5'- ATCCAGTGCAGGGTCCGAGG-3'; U6 F-5'-GTGCTCGCTTCGGCAG CACATAT-3', R- 5'-RAAAATATGGAACGCTTCACGAA-3'), using the CFX96 Touch Thermal Cycler (Bio-Rad, USA) with an initial denaturation at 95 °C for 30 s, followed by 45 cycles of denaturation, primer annealing, and primer extension at 95 °C for 10 s, 60 °C for 30 s, and 72 °C for 5 s, respectively. PCR data were analyzed with the comparative CT method ($2^{-\Delta\Delta CT}$). *Gapdh* and U6 served as internal controls for the mRNA and miRNA analyses, respectively.

Mice and mouse models

Mice

6-week-old C57BL/6 J female mice weighing 19.8 g were purchased from the Laboratory Animal Center of Air Force Medical University, Xi'an, Shaanxi, China, and were maintained in specific-pathogen-free (SPF) conditions with free access to water and feed. All animal experiments were performed in compliance with relevant ethical regulations of the Guiding Principles for the Care and Use of Laboratory Animals (the Institutional Experimental Animal Committee of Northwestern Polytechnical University, Xi'an, China [202000001]) and were approved by the Institutional Experimental Animal Committee of Northwestern Polytechnical University, Xi'an, China.

Osteoporosis OVX mouse model

The OVX mouse model was constructed using 8-week-old female C57BL/6 J mice according to a previously established procedure [40]. Briefly, a single midline dorsal incision was made on the back of anesthetized mice, and subcutaneous connective tissue was freed from the underlying muscle on each side. The ovaries were located under the thin muscles, and by securing a single ligature around the oviduct, the ovaries were removed. The muscle layers and skin incision were sutured. Mice were then kept under observation for a full recovery and then randomly divided into different groups.

Pre-therapeutic evaluation of anti-miR-138-5p delivered by PS to OVX mice

Nine 8-week-old female C57BL/6 J mice were ovariectomized (OVX) and then left untreated for 4 weeks. OVX mice were then divided into three groups: the OVX group, the PS + NC group, and the PS + RNA group. The OVX group received PBS; the PS + NC and PS + RNA groups received 100 μl of PS + NC and PS + antagomir

138-5p, respectively, with an NC or antagomir dose of 1 mg/kg. The mice in each group received four periodic intravenous (tail vein) injections at an interval of 1 week for 4 weeks. Table 1 summarized the experimental groups and dosage administered during the treatment period. After completion of treatment, mice were euthanized, and bones were collected for further analysis (Fig. 6A**).**

Dual-energy X-ray absorptiometry (DXA)

The mice were sedated with pentobarbital sodium (1.2 mg/10 g) and placed on the specimen tray of the DXA body composition analysis system (InAlyzer, Medikors) in a prone position for scanning. Radiographic images as well as related parameters of various bone regions were acquired using InAlyzer Dual X-ray Digital Imaging Software (InAlyzer, Medikors).

Mechanical properties of bone

The mechanical properties of the femur were investigated using a three-point bending test, as previously described [41]. A UniVert (CellScale Biomaterials Testing, Canada) was used to perform a three-point bending test on each femur. The femurs were placed horizontally on two supports spaced 5 mm apart. To load the midpoint of the femur, an accutator was lowered at a speed of 1.0 mm per minute. The bending load was applied continuously until the fracture occurred. Load and displacement data were collected at a 100 Hz sampling rate.

Statistical analyses

The mean ± SD is used to express all statistical data. Unpaired student's t-tests were used to analyze the significant differences between the two groups. Two-way ANOVA was performed to compare the differences among multiple groups followed by Tukey's test.All statistical analyses were performed using GraphPad Prism 7 software. $P < 0.05$ was regarded as statistically significant. For the experiment, significance was defined as $^{*}P < 0.05$, $^{**}P < 0.01$, $^{***}P < 0.001$, and $^{****}P < 0.0001$.

Results and discussion

Synthesis

We designed a functional delivery system having the capabilities of PAMAM (G5) and SDSSD (PS) to deliver the desired gene to osteoblasts, as shown in Fig. 1B**.**

Characterization

Prepared PS nanoparticles were characterized for their size, structural composition, and nucleic acid binding capacity. The shape of the nanoparticle was examined using scanning electron microscopy (SEM), which showed a uniform spherical morphology of the particles (Fig. 2A**).** ^{1}H NMR analysis of PS nanoparticles confirmed the successful attachment of the SDSSD peptide to PAMAM (Fig. 2B).

Furthermore, we used dynamic light scattering (DLS) to determine the size and zeta potential of PS nanoparticles. The average zeta potential of PS was 17.6 mV (Fig. 2C), and the diameter was 217.2 nm (Fig. 2D), suggesting that the prepared particles were stable and could resist flocculation. The agarose gel electrophoresis assay showed that even at the lowest weight ratios of PS/nucleic acid (P/N, wt/wt), i.e., 5:1, PS nanoparticles could impede the migration of nucleic acid (Fig. 2E).

Cytotoxicity

At the cellular level, the MTT assay confirmed the biocompatibility of PS nanoparticles. Compared to PEI, PS nanoparticles demonstrated a high percentage of cell viability at all concentrations, whereas PEI showed a toxic effect on the cell line tested (Fig. 3A-C). Overall, PS proved to be an excellent in vitro biocompatible particle.

Gene silencing ability of PS nanoparticles

We tested whether adding the SDSSD peptide to modified PAMAM had any effect on its gene delivery ability by transfecting HEK293-EGFP cells with GFP siRNA. We observed no significant difference in the reduction in fluorescence between P + GFP siRNA and PS + GFP siRNA-treated cells. Interestingly, we detected a significant reduction in fluorescence in the PS + GFP siRNA group compared to the PEI + siRNA group (Fig. 4A-B**).** This indicates that the attachment of SDSSD to PAMAM had no negative effect on PS's transfection ability.

Table 1 Experimental groups and dosage during treatment

Sr. No	Group	Number of mice	Therapeutic (Dosage)	Duration of Treatment
1	OVX group	3	Saline	4 weeks
2	PS + NC group	3	Negative control with PS (1 mg/kg)	
3	PS + RNA group	3	Antagomir 138-5p with PS (1 mg/kg)	

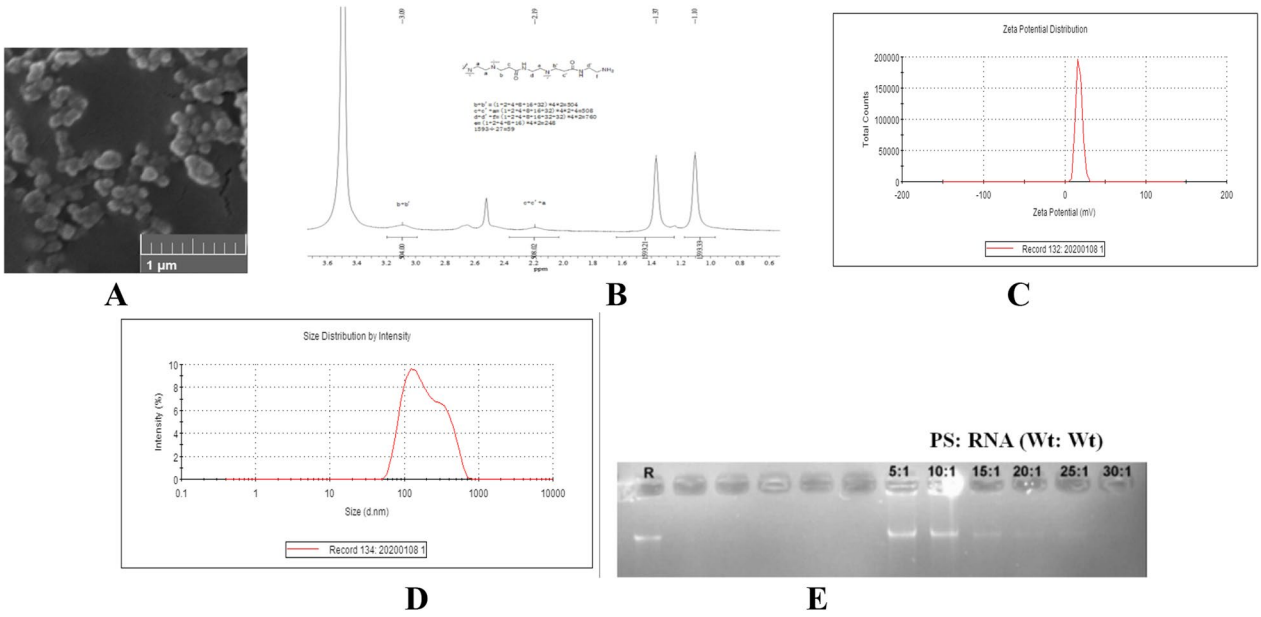

Fig. 2 Characterization of PS nanoparticles: **A** A typical image of a scanning electron micrograph of PS (scale bar: 1 µm). **B** ^{1}H NMR spectrum of PS. **C** Zeta potential of PS determined by dynamic light scattering. **D** The particle size distribution of PS. **E** The binding capacity of PS to miR-138-5p measured by an electrophoretic mobility assay

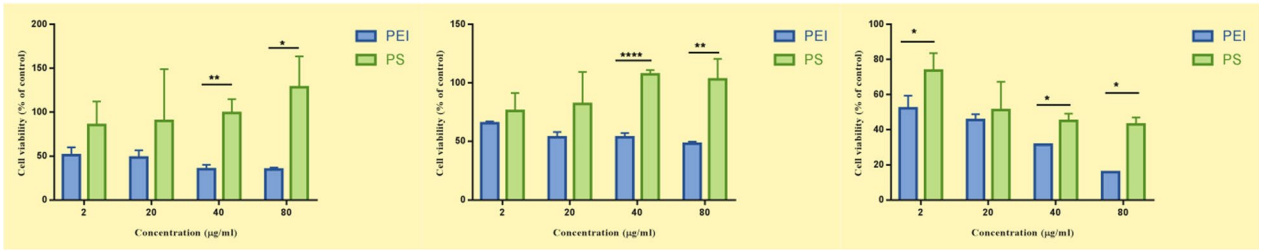

Fig. 3 Biocompatibility and gene silencing ability of PS nanoparticles. Cytotoxic effect of different concentrations of PS and PEI on different cell lines using the MTT assay after 24 h of incubation; **A** MC3T3-E1 cell line; **B** RAW 264.7 cell line; and **C** C3H10T1/2 cell line. All data are shown as mean ± SD, $n = 3$. A student's t-test was used to compare the differences between the two groups. *$P < 0.05$, **$P < 0.01$, and ****$P < 0.0001$ *vs*. PEI. (PS: SDSSD-modified PAMAM; PEI: Polyethylenimine)

In vitro RNA delivery ability in osteoblasts

The specificity of SDSSD-modified PAMAM was also examined towards osteoblast. The osteoblast-specific RNA delivery capacity of PS particles was investigated by using mouse pre-osteoblast MC3T3-E1 and leukemic monocyte/macrophage RAW264.7 cell lines. Previous research has found that miR-138-5p targets microtubule actin crosslinking factor 1 (MACF1), which is involved in osteoblast differentiation, and thus negatively regulates osteoblast differentiation and bone formation [42, 43]. Therefore, PS nanoparticles were used to deliver antagomir 138-5p to investigate its potential as a bone anabolic therapy for osteoporosis.

Cells were incubated with PS nanoparticles with antagomir 138-5p, and after 24 h, the ability of PS nanoparticles to deliver antagomir 138-5p in osteoblasts and osteoclasts was determined by measuring the relative expression of miR 138-5p and its target gene, MACF1, using qPCR. The data showed a significant reduction in the expression of miR 138-5p (Fig. 5A) and increased levels of microtubule-actin crolinking factor 1 (MACF1) in MC3T3-E1 cells treated with PS + antagomir 138-5p compared to non-modified nanoparticles with antagomir 138-5p (Fig. 5B). However, no such significant correlation was observed in the RAW 264.7 cell

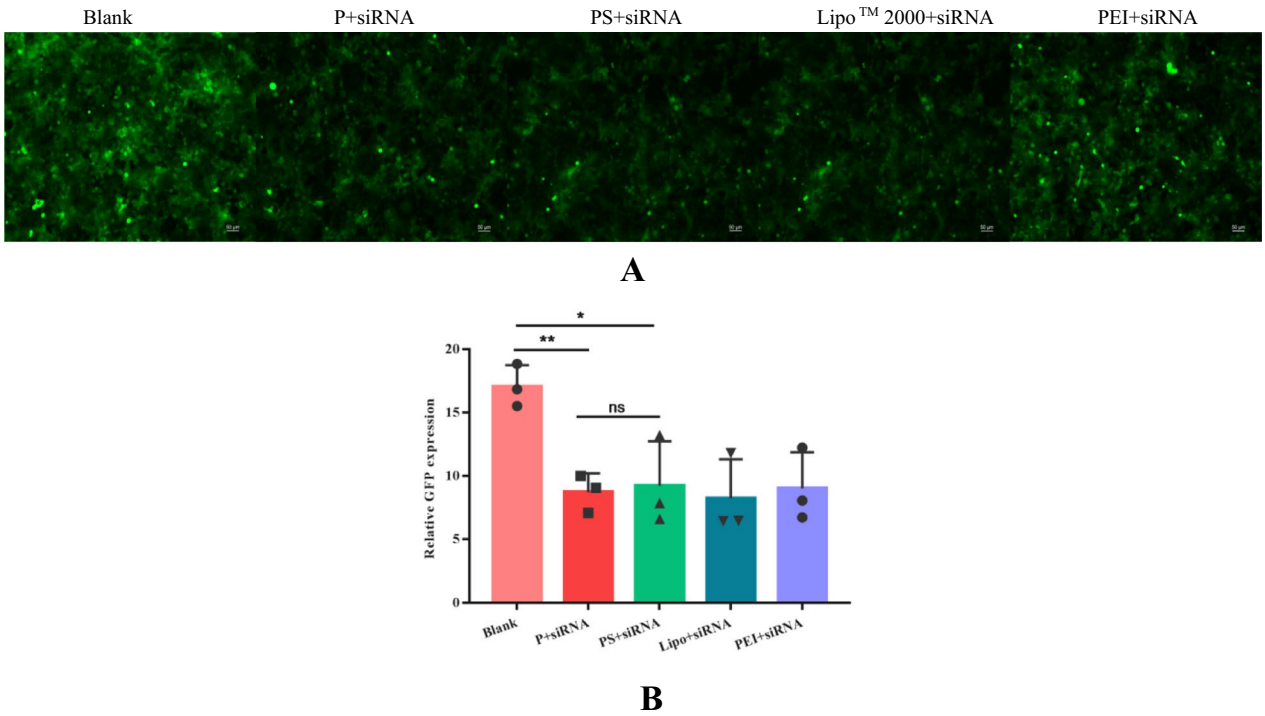

Fig. 4 Gene silencing ability of PS nanoparticles in HEK293-EGFP cells transfected with GFP siRNA. **A** Fluorescent microscopy images of HEK293-EGFP cells transfected with GFP siRNA using P, Lipofectamine™ 2000 (Lipo™ 2000), and PEI. Lipofectamine™ 2000 (Lipo™ 2000), and PEI-treated groups served as positive controls (scale bar: 50 µm). **B** Semi-quantified analysis of green channel images using ImageJ software. Data are represented as mean ± SD, $n = 3$. A student's t-test was used to compare the differences between the two groups. *$P < 0.05$, **$P < 0.01$ *vs.* blank. (P + siRNA: PAMAM + GFP siRNA; PS + RNA: SDSSD-modified PAMAM + GFP siRNA; Lipo + siRNA: Lipofectamine™ 2000 + GFP siRNA; PEI + siRNA: Polyethylenimine + GFP siRNA; ns: not significant)

line (Fig. 5C and D), indicating their ability to deliver antagomir 138-5p preferentially to osteoblasts.

In vivo delivery ability and mechanical properties of bone

Based on the results of in vitro research, we performed a preliminary therapeutic investigation of PS + antagomir 138-5p in OVX mice. After receiving injections through the tail vein once a week for four weeks, mice were subjected to DXA InAlyzer analysis to acquire radiographic images as well as related parameters of various bone regions. In comparison to OVX and PS + NC, the distal tibia and femur of mice that received repeated injections of PS + antagomir 138-5p showed a significant increase in the BMD (Fig. 6B and C), BMC (Fig. 6D), and bone volume (Fig. 6E).

The mechanical characteristics of mouse femurs, including stress and elasticity, were then tested using a three-point bending test to see if the improved BMD also improved bone strength. It was found that a greater force was required to achieve the end result (break in the femurs) in the femurs of mice in the PS + RNA group than in the OVX or PS + NC groups (Fig. 7A). Additionally, compared to the femurs of OVX or PS + NC group mice, the femurs from PS + RNA group mice were able to withstand higher stress (Fig. 7B) and displayed a higher modulus of elasticity (Fig. 7C), indicating that they were stiffer and more force-resistant. However, PS + NC groups showed no significant value when compared to the OVX group. Therefore, it suggests that these nanoparticles could deliver antagomir 138-5p in vivo and improve bone health in OVX mice.

Discussion

Polymers have evolved as strong candidates to facilitate nucleic acid delivery to various cells, but their cytotoxicity and inability to specifically deliver the cargo often hamper their broader application, and in such cases, modifications can provide the answer. Much work on polymer modification with peptides has shown their capability to specifically deliver nucleic acids to cells without having any significant toxicity. One such peptide is Ser-Asp-Ser-Asp (SDSSD), which has been demonstrated to possess a high affinity for osteoblast-specific factor 2 (OSF-2) and thus can specifically target osteoblasts [37, 44]. PAMAM modification with SDSSD demonstrated that these nanoparticles were

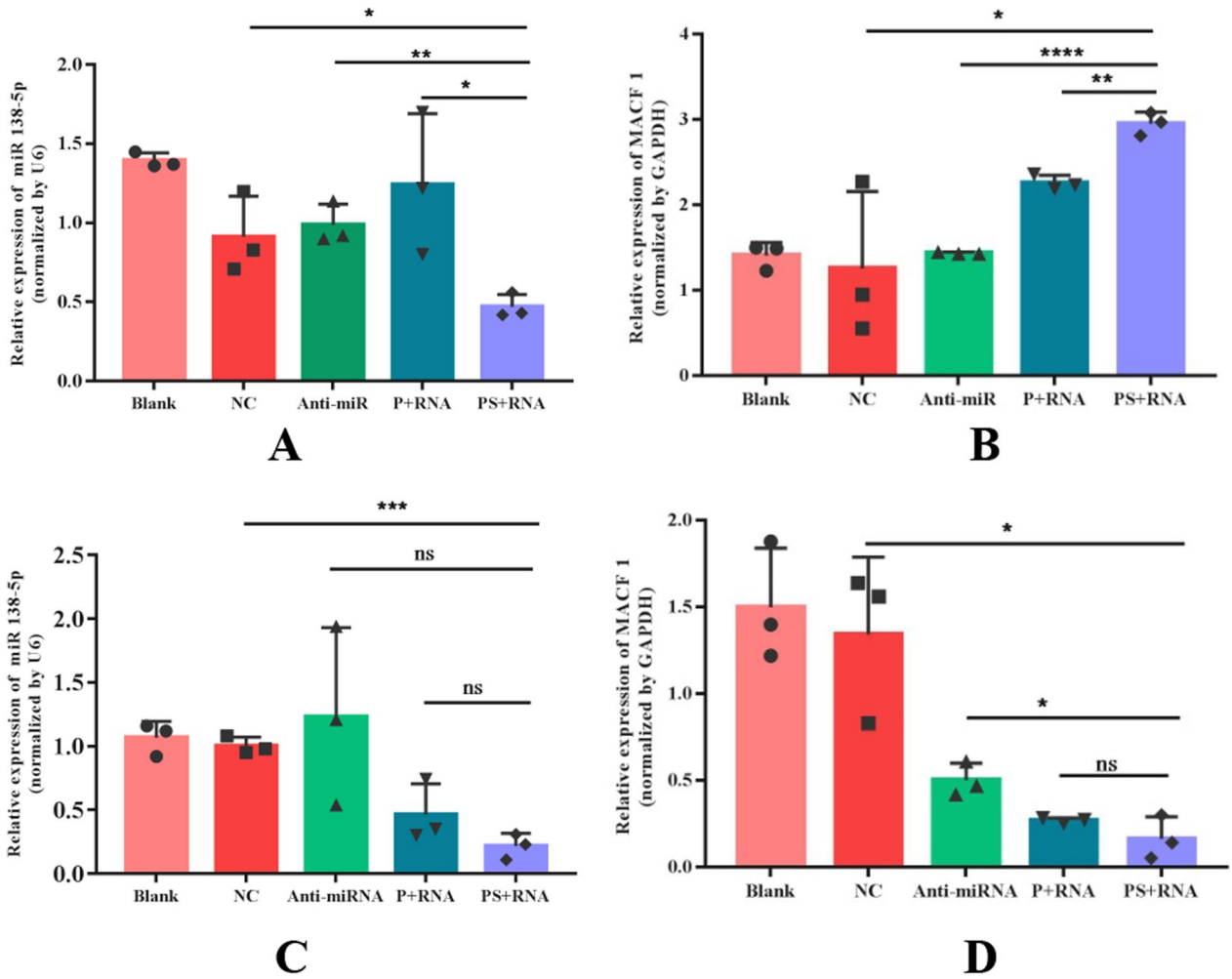

Fig. 5 In vitro targeting and delivery ability of PS nanoparticles. **A** Relative expression of miR-138-5p and **B** its target gene, MACF1, in the MC3T3-E1 cell line. **C** Relative expression of miR-138-5p and **D** its target gene, MACF1, in the RAW 264.7 cell line. U6 and GAPDH were the internal controls for 138-5p and MACF1, respectively. Data are shown as mean ± SD, n = 3. A student's t-test was used to compare the differences between the two groups. *$P < 0.05$, **$P < 0.01$, ***$P < 0.001$, ****$P < 0.0001$ *vs.* P + RNA. (RNA: Antagomir 138-5p; P + RNA: PAMAM (without SDSSD) + Antagomir 138-5p; PS + RNA: SDSSD-modified PAMAM + Antagomir 138-5p; Anti-miRNA: Antagomir 138-5p; ns: not significant)

biocompatible and could specifically target and deliver antagomir 138-5p into osteoblast cells, as evidenced by qPCR results. Previous research suggested that internalization could have occurred via a periostin-mediated mechanism [37]. Our in vivo study shows that BMD and bone strength were improved by the injection of RNA with these nanoparticles. These results indicate that PS nanoparticles could deliver antagomir 138-5p in vivo and alleviate osteoporotic symptoms.

This study, however, was limited to in vitro and preliminary in vivo investigations. As a result, we were unable to assess the ability of PS nanoparticles to target osteoblasts in vivo at this time. We would like to emphasize that the delivery system's targeting and delivery capabilities were evaluated quantitatively (qPCR).

Conclusion

In conclusion, we demonstrate that a novel gene delivery system could be developed by modifying PAMAM with the SDSSD peptide. This preliminary study shows that PS nanoparticles could target and selectively deliver RNA to osteoblasts in vitro and alleviate osteoporotic symptoms in vivo. As a result, the findings of this study suggest that PS nanoparticles could be a potentially safe and effective delivery system for osteoblasts. Based on these findings, more in-depth in vivo analysis experiments are needed to evaluate and establish its potential as a therapeutic delivery system for treating bone disorders.

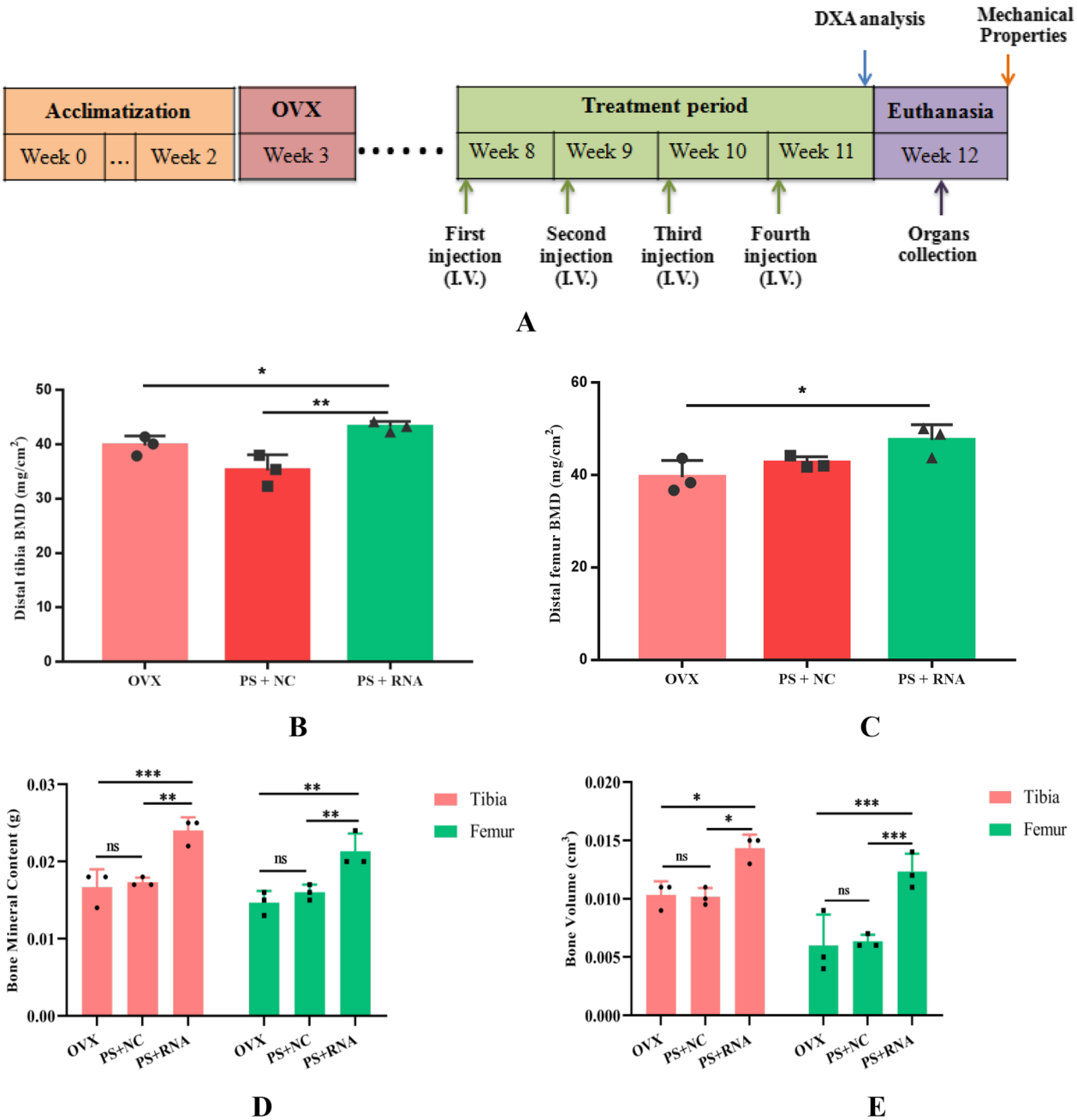

Fig. 6 In vivo targeting and delivery ability of PS nanoparticles. **A** A schematic diagram illustrating the experimental design. **B** BMD of distal tibia, and **C** BMD of distal femur. **D** BMC of distal tibia and femur. **E** Bone volume of distal tibia and femur. A student's t-test was used to compare the differences between the two groups. Two-way ANOVA was performed to compare the differences among multiple groups followed by Tukey's test. Data are shown as mean ± SD, n = 3. **P* < 0.05, ***P* < 0.01, ****P* < 0.001 *vs*. OVX or PS + NC. (PS + NC: SDSSD-modified PAMAM + Negative Control; PS + RNA: SDSSD-modified PAMAM + Antagomir 138-5p)

Future prospects

Given the amount of research that is being carried out to understand the effects of RNA in healthy as well as disease states, their potential as RNA therapeutics has become an interesting area of research. However, RNA alone is not efficient enough to impart therapeutic effects when administered, and therefore, delivery systems need to be developed to transport RNAs. This study, though limited to preliminary in vivo investigations, has shown promising results so far. To establish

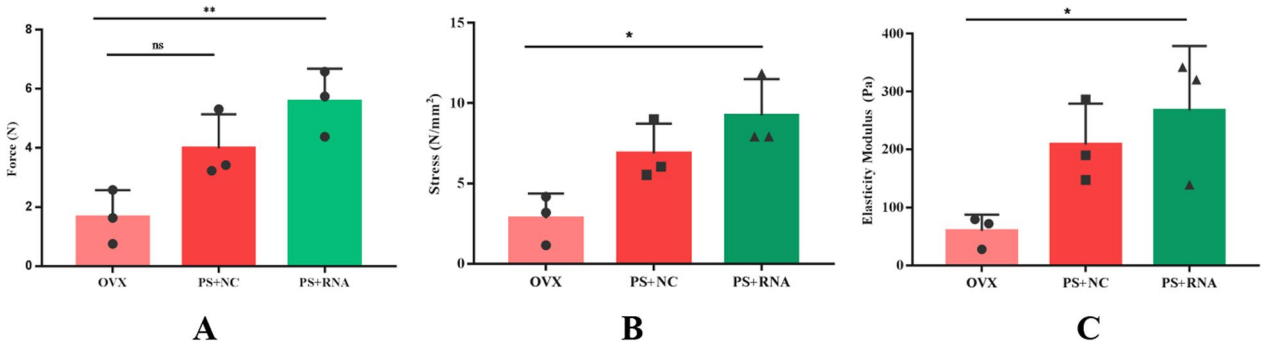

Fig. 7 The mechanical properties of the femur. **A** Three-point bending measurement of maximum force in femurs of OVX, PS + NC, and PS + RNA group mice demonstrating force-resistance in PS + RNA group compared to OVX and PS + NC groups. **B** Three-point bending measurement of stress in femurs of OVX, PS + NC, and PS + RNA group mice, indicating higher force-resistance of the femurs from PS + RNA. **C** Three-point bending measurement of elasticity modulus in femurs of OVX, PS + NC, and PS + RNA group mice, showing higher modulus of elasticity of PS + RNA group mice femurs. A student's t-test was used to compare the differences between the two groups. Data are shown as mean ± SD, $n = 3$. $^{*}P < 0.05$ $^{**}P < 0.01$ *vs*. OVX mice. (PS + NC: SDSSD-modified PAMAM + Negative Control; PS + RNA: SDSSD-modified PAMAM + Antagomir 138-5p; ns: not significant)

SDSSD-modified polymers as an effective bone-targeting system, their pharmacokinetic profile needs to be established to determine the exact dosage interval needed to achieve maximum therapeutic effect without toxicity. Moreover, the establishment of various mouse models, such as osteosarcoma or osteopenia, could provide insight into the pharmacodynamic properties of the PS nanoparticles. Additionally, more in-depth effects of the nucleic acid delivery abilities of PS nanoparticles can be assessed through micro-computed tomography to analyze trabecular as well as cortical structure and through immunohistochemistry.

All animal experiments were performed in compliance with relevant ethical regulations of the Institutional Experimental Animal Committee of Northwestern Polytechnical University, Xi'an, China. Ethical Approval Number – 202,000,001.

Abbreviations

ASO	Antisense oligonucleotide
ATCC	American type culture collection
BMC	Bone mineral content
BMD	Bone mineral density
CT	Computed tomography
D_2O	Deuterium oxide
DIPEA	Diisopropylethylamine
DLS	Dynamic light scattering
DMEM	Dulbecco's modified eagle medium
DMSO	Dimethyl sulfoxide
DNA	Deoxyribonucleic acid
DXA	Dual-energy X-ray absorptiometry
EDCI	1-Ethyl-3-(3-dimethylaminopropyl) carbonyldiimide hydrochloride
EDTA	Ethylenediaminetetraacetic acid
EGFP	Enhanced green fluorescent protein
FBS	Fetal bovine serum
GAPDH	Glyceraldehyde-3-phosphate dehydrogenase
GFP	Green fluorescent protein
HOBt	1-Hydroxybenzotriazole
MACF1	Microtubule actin crosslinking factor 1
MEM	Minimal essential medium
MTT	3-(4, 5-Dimethylthiazolyl-2)-2, 5-diphenyltetrazolium bromide
NC	Negative control
NMR	Nuclear magnetic resonance
OSF-2	Osteoblast-specific factor 2
OVX	Overiectomy
PAMAM	Polyamidoamine
PBS	Phosphate buffer saline
PCR	Polymerase chain reaction
PDI	Polydispersity index
PEG	Polyethylene glycol
PEI	Polyethylenimine
PS	SDSSD modified PAMAM (PAMAM-SDSSD)
PTH	Parathyroid hormone
RBC	Red blood cells
RGD	Arginine-glycine-aspartate
RNA	Ribonucleic acid
RT	Room temperature
SD	Standard deviation
SDSSD	Serine-aspartate-serine-serine-serine-aspartate
SEM	Scanning electron microscope
SERM	Selective estrogen receptor modulator
SPF	Specific-pathogen-free
TAE	Tris acetate EDTA
TFA	Trifluoroacetic acid

Acknowledgements
The authors would like to express gratitude to Dr. Hong Zhou (The University of Sydney, Australia) for generously providing the MC3T3-E1 cell line.

Author contributions
SP: Conceptualization, Methodology, Data curation, Investigation, Writing-original draft, Writing-review & editing. YGG: Conceptualization, Methodology, Supervision, Writing-review & editing. AQ: Writing-review & editing, Funding acquisition, Resources, Validation, Supervision.

Funding
This work was funded by the Fundamental Research Funds for the Central Universities (grant number D5000210746), Natural Science Foundation of Hebei Province (No. 2021105001).

Availability of data and materials
The data that support the findings of this study are available from the corresponding author upon a reasonable request.

Declarations

Ethics approval and consent to participate
All animal experiments were performed in compliance with relevant ethical regulations of the Guiding Principles for the Care and Use of Laboratory Animals (the Institutional Experimental Animal Committee of Northwestern Polytechnical University, Xi'an, China [202000001]) and were approved by the Institutional Experimental Animal Committee of Northwestern Polytechnical University, Xi'an, China.

Consent for publication
The authors declare no conflict of interest**.**

Competing interests
The authors declare no competing interest.

Received: 12 February 2023 Accepted: 14 November 2023
Published online: 21 November 2023

References

1. Barbosa JS, Mendes RF, Figueira F, Gaspar VM, Mano JF, Braga SS, Rocha J, Almeida Paz FA (2020) Bone tissue disorders: healing through coordination chemistry. Chemistry 26(67):15416–15437
2. Aspray TJ, Hill TR (2019) Osteoporosis and the ageing skeleton. Subcell Biochem 91:453–476
3. Cawthray J, Wasan E, Wasan K (2017) Bone-seeking agents for the treatment of bone disorders. Drug Deliv Transl Res 7(4):466–481
4. (2021) Management of osteoporosis in postmenopausal women: the 2021 position statement of The North American Menopause Society. Menopause 28(9):973-997
5. Yong EL, Logan S (2021) Menopausal osteoporosis: screening, prevention and treatment. Singapore Med J 62(4):159–166
6. Gao Y, Patil S, Jia J (2021) The development of molecular biology of osteoporosis. Int J Mol Sci 22(15):8182
7. Vandamme C, Adjali O, Mingozzi F (2017) Unraveling the complex story of immune responses to AAV vectors trial after trial. Hum Gene Ther 28(11):1061–1074
8. Paunovska K, Loughrey D, Dahlman JE (2022) Drug delivery systems for RNA therapeutics. Nat Rev Genet 23(5):265–280
9. Patil S, Gao Y-G, Lin X, Li Y, Dang K, Tian Y, Zhang W-J, Jiang S-F, Qadir A, Qian A-R (2019) The development of functional non-viral vectors for gene delivery. Int J Mol Sci 20(21):5491
10. Jayant RD, Sosa D, Kaushik A, Atluri V, Vashist A, Tomitaka A, Nair M (2016) Current status of non-viral gene therapy for CNS disorders. Expert Opin Drug Deliv 13(10):1433–1445
11. Zu HG (2021) Non-viral vectors in gene therapy: recent development, challenges, and prospects. Aaps j 23(4):78
12. Chen CK, Huang PK, Law WC, Chu CH, Chen NT, Lo LW (2020) Biodegradable polymers for gene-delivery applications. Int J Nanomedicine 15:2131–2150
13. Tian Y, Zhao Y, Yin C, Tan S, Wang X, Yang C, Zhang T-D, Zhang X, Ye F, Xu J, Wu X, Ding L, Zhang J, Pei J, Wang X-T, Zhang RX, Xu J, Wang W, Filipe CDM, Hoare T, Yin D-C, Qian A, Deng X (2022) Polyvinylamine with moderate binding affinity as a highly effective vehicle for RNA delivery. J Control Release 345:20–37
14. Zou Y, Li D, Shen M, Shi X (2019) Polyethylenimine-based nanogels for biomedical applications. Macromol Biosci 19(11):e1900272
15. Dias AP, da Silva SS, da Silva JV, Parise-Filho R, Igne Ferreira E, Seoud OE, Giarolla J (2020) Dendrimers in the context of nanomedicine. Int J Pharm 573:118814
16. Chauhan AS (2018) Dendrimers for Drug Delivery. Molecules 23(4).
17. Chis AA, Dobrea C, Morgovan C, Arseniu AM, Rus LL, Butuca A, Juncan AM, Totan M, Vonica-Tincu AL, Cormos G, Muntean AC, Muresan ML, Gligor FG, Frum A (2020) Applications and limitations of dendrimers in biomedicine. Molecules 25(17):3982
18. Abedi-Gaballu F, Dehghan G, Ghaffari M, Yekta R, Abbaspour-Ravasjani S, Baradaran B, Dolatabadi JEN, Hamblin MR (2018) PAMAM dendrimers as efficient drug and gene delivery nanosystems for cancer therapy. Appl Mater Today 12:177–190
19. Tang Y, Li YB, Wang B, Lin RY, van Dongen M, Zurcher DM, Gu XY, Banaszak Holl MM, Liu G, Qi R (2012) Efficient in vitro siRNA delivery and intramuscular gene silencing using PEG-modified PAMAM dendrimers. Mol Pharm 9(6):1812–1821
20. Li G, Zhang Y, Tang W, Zheng J (2020) Comprehensive investigation of in vitro hemocompatibility of surface modified polyamidoamine nanocarrier. Clin Hemorheol Microcirc 74(3):267–279
21. Pishavar E, Attaranzadeh A, Alibolandi M, Ramezani M, Hashemi M (2018) Modified PAMAM vehicles for effective TRAIL gene delivery to colon adenocarcinoma: in vitro and in vivo evaluation. Artif Cells Nanomed Biotechnol 46(sup3):S503-s513
22. Saito G, Velluto D, Resmini M (2018) Synthesis of 1,8-naphthalimide-based probes with fluorescent switch triggered by flufenamic acid. Royal Society Open Sci 5(6):172137
23. Choi S-A, Park CS, Kwon OS, Giong H-K, Lee J-S, Ha TH, Lee C-S (2016) Structural effects of naphthalimide-based fluorescent sensor for hydrogen sulfide and imaging in live zebrafish. Sci Rep 6(1):26203
24. Gao Y-G, Tang Q, Shi Y-D, Zhang Y, Lu Z-L (2016) 1,8-Naphthalimide modified [12]aneN3 compounds as selective and sensitive probes for Cu2+ ions and ATP in aqueous solution and living cells. Talanta 152:438–446
25. Gao YG, Liu FL, Patil S, Li DJ, Qadir A, Lin X, Tian Y, Li Y, Qian AR (2019) 1,8-Naphthalimide-based multifunctional compounds as Cu(2+) probes, lysosome staining agents, and non-viral vectors. Front Chem 7:616
26. Carbone EJ, Rajpura K, Allen BN, Cheng E, Ulery BD, Lo KW (2017) Osteotropic nanoscale drug delivery systems based on small molecule bone-targeting moieties. Nanomedicine 13(1):37–47
27. Liang C, Guo B, Wu H, Shao N, Li D, Liu J, Dang L, Wang C, Li H, Li S, Lau WK, Cao Y, Yang Z, Lu C, He X, Au DWT, Pan X, Zhang B-T, Lu C, Zhang H, Yue K, Qian A, Shang P, Xu J, Xiao L, Bian Z, Tan W, Liang Z, He F, Zhang L, Lu A, Zhang G (2015) Aptamer-functionalized lipid nanoparticles targeting osteoblasts as a novel RNA interference–based bone anabolic strategy. Nat Med 21(3):288–294
28. Wang D, Miller SC, Shlyakhtenko LS, Portillo AM, Liu XM, Papangkorn K, Kopecková P, Lyubchenko Y, Higuchi WI, Kopecek J (2007) Osteotropic peptide that differentiates functional domains of the skeleton. Bioconjug Chem 18(5):1375–1378
29. Yarbrough DK, Hagerman E, Eckert R, He J, Choi H, Cao N, Le K, Hedger J, Qi F, Anderson M, Rutherford B, Wu B, Tetradis S, Shi W (2010) Specific binding and mineralization of calcified surfaces by small peptides. Calcif Tissue Int 86(1):58–66
30. Zhang G, Guo B, Wu H, Tang T, Zhang B-T, Zheng L, He Y, Yang Z, Pan X, Chow H, To K, Li Y, Li D, Wang X, Wang Y, Lee K, Hou Z, Dong N, Li G, Leung K, Hung L, He F, Zhang L, Qin L (2012) A delivery system targeting bone formation surfaces to facilitate RNAi-based anabolic therapy. Nat Med 18(2):307–314
31. Gao Y, Patil S, Qian A (2020) The role of MicroRNAs in bone metabolism and disease. Int J Mol Sci 21(17):6081
32. Patil S, Dang K, Zhao X, Gao Y, Qian A (2020) Role of LncRNAs and CircRNAs in Bone Metabolism and Osteoporosis. Front Gen 11.
33. Feng R, Patil S, Zhao X, Miao Z, Qian A (2021) RNA therapeutics - research and clinical advancements. Front Mol Biosci 8:710738
34. Wang P, Perche F, Logeart-Avramoglou D, Pichon C (2019) RNA-based therapy for osteogenesis. Int J Pharm 569:118594
35. Hu B, Zhong L, Weng Y, Peng L, Huang Y, Zhao Y, Liang XJ (2020) Therapeutic siRNA: state of the art. Signal Transduct Target Ther 5(1):101
36. Singh A, Trivedi P, Jain NK (2018) Advances in siRNA delivery in cancer therapy. Artif Cells Nanomed Biotechnol 46(2):274–283
37. Sun Y, Ye X, Cai M, Liu X, Xiao J, Zhang C, Wang Y, Yang L, Liu J, Li S, Kang C, Zhang B, Zhang Q, Wang Z, Hong A, Wang X (2016) Osteoblast-targeting-peptide modified nanoparticle for siRNA/microRNA delivery. ACS Nano 10(6):5759–5768
38. Gao YG, Huangfu SY, Patil S, Tang Q, Sun W, Li Y, Lu ZL, Qian A (2020) [12]aneN(3)-based multifunctional compounds as fluorescent probes and nucleic acids delivering agents. Drug Deliv 27(1):66–80
39. Gao YG, Alam U, Ding AX, Tang Q, Tan ZL, Shi YD, Lu ZL, Qian AR (2018) [12]aneN(3)-based lipid with naphthalimide moiety for enhanced gene transfection efficiency. Bioorg Chem 79:334–340

40. Idris AI, *Ovariectomy/Orchidectomy in Rodents*, in *Bone Research Protocols*, M.H. Helfrich and S.H. Ralston, Editors. 2012, Humana Press: Totowa, NJ.545–551.
41. Osuna LGG, Soares CJ, Vilela ABF, Irie MS, Versluis A, Soares PBF (2020) Influence of bone defect position and span in 3-point bending tests: experimental and finite element analysis. Braz Oral Res 35:e001
42. Chen Z, Zhao F, Liang C, Hu L, Li D, Zhang Y, Yin C, Chen L, Wang L, Lin X, Su P, Ma J, Yang C, Tian Y, Zhang W, Li Y, Peng S, Chen W, Zhang G, Qian A (2020) Silencing of miR-138-5p sensitizes bone anabolic action to mechanical stimuli. Theranostics 10(26):12263–12278
43. Chen Z, Huai Y, Chen G, Liu S, Zhang Y, Li D, Zhao F, Chen X, Mao W, Wang X, Yin C, Yang C, Xu X, Ru K, Deng X, Hu L, Li Y, Peng S, Zhang G, Lin X, Qian A (2022) MiR-138-5p targets MACF1 to aggravate aging-related bone loss. Int J Biol Sci 18(13):4837–4852
44. Liu M, Zhu D, Jin F, Li S, Liu X, Wang X (2023) Peptide modified genipo-sidic acid targets bone and effectively promotes osteogenesis. J Orthop Translat 38:23–31

Publisher's Note